Bioorganic Chemistry 39 (2011) 59–66

Contents lists available at ScienceDirect

Bioorganic Chemistry

journal homepage: www.elsevier.com/locate/bioorg

High resolution NMR conformational studies of new bivalent NOP receptor antagonists in model membrane systems

Anna Borioni [a,*], Giuditta Bastanzio [b], Maurizio Delfini [b], Carlo Mustazza [a], Fabio Sciubba [c], Massimo Tatti [d], Maria Rosaria Del Giudice [a]

[a] Istituto Superiore di Sanità, Dipartimento del Farmaco, Viale Regina Elena 299, 00161 Roma, Italy
[b] Università degli studi di Roma La Sapienza, Dipartimento di Chimica, Piazzale Aldo Moro 5, 00185 Roma, Italy
[c] Università Telematica Internazionale Uninettuno, Facoltà di Ingegneria, Corso Vittorio Emanuele II 39, 00186 Roma, Italy
[d] Istituto Superiore di Sanità, Dipartimento di Ematologia, Oncologia e Medicina molecolare, Viale Regina Elena 299, 00161 Roma, Italy

ARTICLE INFO

Article history:
Received 11 November 2010
Available online 17 December 2010

Keywords:
Opioid antagonists
Quinoline derivatives
Micelles
Liposomes
NMR

ABSTRACT

The interaction of new bivalent NOP receptor antagonists with dodecyl phosphatidylcholine micelles and DMPC/cholesterol liposomes was investigated in solution by high resolution NMR. The ligands are structurally related to the NOP antagonist JTC-801 plus a propanediamine or heptanediamine spacer between the pharmacophoric units. Ligand internuclear distances were derived from 2D NOESY data and applied to molecular modelling calculations as conformational restraints. NMR experiments on micelles evidenced that the ligands closely approached the micelles but gave no hints on the preferential conformations of the interacting ligands. Results from NMR experiments in the presence of liposomes clearly indicated that both ligands strongly interacted with the bilayer assuming a preferential folded conformation with the quinoline arms superimposing on each other. The finding suggested that these strongly lipophilic pharmacophores could localize in the native receptorial membrane in the form of a depot, gaining access to the recognition site via the lipid bilayer.

1. Introduction

The Nociceptin Opioid receptor (NOPr) [1] is the most recently discovered member of the family of the opioid receptors. The present rapidly growing pharmacological interest in NOPr antagonists is accounted by their potential clinical applications as analgesics devoid of tolerance, anorexiants, memory enhancers, antidepressants and in the treatment of Parkinson's disease [2]. Further investigations about the possibility that NOP receptors arrange in supramolecular homo and heterodimeric structures similarly to the other members of the opioid receptor family could open new pharmacological perspectives [3]. Indeed activation of dimer receptors proved to elicit completely different cellular response in respect to the monomer [4]. Dimer receptors are supposed to be activated by bivalent ligands. In this view the synthesis and the characterization of bivalent ligands could be a start to verify receptor dimerization. In the case of the opioid receptors that are widely distributed in the nervous systems bivalent ligands were exploited in order to achieve selectivity among central and peripheral effects [5]. In fact, though binding to the same receptor, they often displayed different Blood–Brain Barrier permeation in respect to the monomeric unit.

On a general base it can be assumed that the ligand/receptor interaction is driven, as a first step, by the contact of the ligand with the lipids of the cellular membrane and then by lateral diffusion within the membrane leaflet. In this paper we aimed at collecting hints on the conformational status of bivalent NOP antagonists in interaction with the receptor membrane. In particular, information on the distances among chemical groups within the same molecule could suggest if the ligands may elongate to reach possible different receptorial units. In this view, a study of the ligands in solution together with lipophilic membrane models was first approached [6]. We employed NMR spectroscopy to assess the spatial arrangement of the ligands in interaction with the membrane models as this technique provides information on molecular structures at atomic level and it is sensitive to dynamic parameters in solution [7]. In particular we performed 2D NOESY NMR experiments to evaluate the Nuclear Overhauser Effect (NOE) that is depending on the molecular inter-protonic distances [8,9].

The bivalent ligands selected for this study were synthesized in our laboratory as new derivatives of the NOP antagonist JTC-801 [*N*-(4-amino-2-methylquinolin-6-yl)-2-(4-ethylphenoxymethyl)-benzamide]. This molecule was the first NOP antagonist used in

* Corresponding author. Fax: +39 0649902516.
E-mail address: anna.borioni@iss.it (A. Borioni).

0045-2068/$ - see front matter © 2010 Elsevier Inc. All rights reserved.
doi:10.1016/j.bioorg.2010.12.001

clinical trials and showed a peculiar pharmacological behaviour possibly binding to an allosteric site of the NOP receptor [10–12]. At present time no other dimeric non-peptidic NOPr ligands are known with the only exception of a class of spiropiperidine agonists patented by Clark & Elbing LLP [13].

The bivalent ligands here under investigation are structured as two identical pharmacophoric moieties mainly corresponding to JTC-801 spaced by a diaminopropane or a diaminoheptane chain (Fig. 1). They are sized 864 and 920 Da and belong to a series of new bivalent NOPr ligands containing aminic and iminic spacers ranging from three to 10 carbon atoms. L3 and L7 showed good chemical stability in the aqueous micellar and liposome environment and good antagonistic activity at the NOP receptor respectively displaying IC_{50} affinity 30 and 31 nM (unpublished data). We chose these compounds as representative of a short spaced molecule (L3) and of a more flexible molecule, which could display various conformations (L7). We mimicked cellular membranes by a micelle model composed by dodecylphosphatidylcholine (DPC). DPC micelles can adequately represent cellular membrane domain displaying high fluidity and permitted to evaluate ligand properties in an environment representing both the inner lipophilic bilayer and the charged outer interface. Investigation of the NMR profile of the ligands in the presence of micelles was performed by ^{1}H 1D and 2D NMR experiments. The study results encouraged the research towards a more complex cellular model represented by unilamellar 1,2-dimyristoyl-3-*sn*-glycerophosphocoline (DMPC)/cholesterol liposomes which could confirm interaction from a different aspect.

Liposomes have more rigid, larger structures compared to micelles, and they also possess an inner hydrophilic cavity potentially able to encapsulate small molecules. Therefore, in some respect they can be more similar than micelles to the expected interaction environment. 2D NOESY data allowed monitoring of distances of molecular moieties within the ligand structure in the presence of liposomes [14].

Finally, distances from NMR experiments were used as restraints in the subsequent molecular modelling to predict the dominant conformations of the ligand in solution in interaction with the molecular membrane model.

2. Materials and methods

2.1. Ligand preparation

Ligands were synthesized in our laboratory [15]. Their structure was unambiguously assigned by ^{1}H NMR, 2D TOCSY, NOESY and ROESY experiments.

2.2. Micelle preparation

Dodecylphosphocholine (18.45 mg, 0.0525 mmol) was dissolved in phosphate buffer 10 mM (0.630 mL) and deuterated DMSO-d_6 (0.070 mL) to a 75 mM concentration which is the well above the critical micellar concentration reported in literature for DPC in similar systems (1.1 mM) [16,17].

2.3. Liposome preparation

Large unilamellar vesicles were prepared from 1,2-dimyristoyl-3-*sn*-glycerophosphocoline (DMPC) and cholesterol (Chol), in 8:2 M ratio.

A DMPC (10.85 mg, 0.016 mmol)/chol (1.55 mg, 0.004) solution in methanol (1 mL) was dried in vacuo for 8 h. The dried and thin lipid film was hydrated at 308 K in deuterated sodium phosphate buffer 10 mM at pH 7.2 (2 mL). The suspension was vortex mixed two times at low rpm for 1 min waiting for an interval of 15 min at 310 K to produce a multilamellar preparation. The lipid dispersion was submitted to 10 freeze–thaw cycles and then it was extruded 21 times through polycarbonate filters (pore size 200 nm) at room temperature by using a LiposoFast System (Avestin). An aliquot of large unilamellar vesicles (0.630 mL) was added to a solution of L7 5 mM in 0.07 mL of DMSO-d_6) so that the final ligand concentration was 0.5 mM in DMSO-d_6/phosphate buffer 10 mM 10:90. This preparation was incubated overnight at 308 K before NMR experiments.

2.4. NMR experiments

1D NMR spectra were acquired on a broad band NMR Bruker Avance 700 MHz. 2D NMR spectra were acquired on an NMR Bruker Avance 400 MHz. The spectrometers are equipped with temperature controller and *z* gradient coils. During acquisition the temperature was maintained at 308 K.

In reference spectra 50% DMSO-d_6/deuterated aqueous phosphate buffer 10 mM at pH 7.2 was employed as solvent. The phosphate buffer contained TSP 0.5 mM as a reference. The appropriate quantity of ligand was dissolved in DMSO-d_6 and deuterated aqueous phosphate buffer 10 mM was added to reach concentrations of the ligand ranging from 0.05 to 1 mM.

2.4.1. NMR experiments in the presence of micelles

A solution of the appropriate ligand in DMSO-d_6 was added to a 75 mM solution of DPC in 10 mM deuterated phosphate buffer to reach a final concentration of 0.5 mM ligand in 10% DMSO-d_6/phosphate buffer. 1D ^{1}H NMR spectra were acquired on a broad band NMR Bruker Avance 700 MHz equipped with temperature

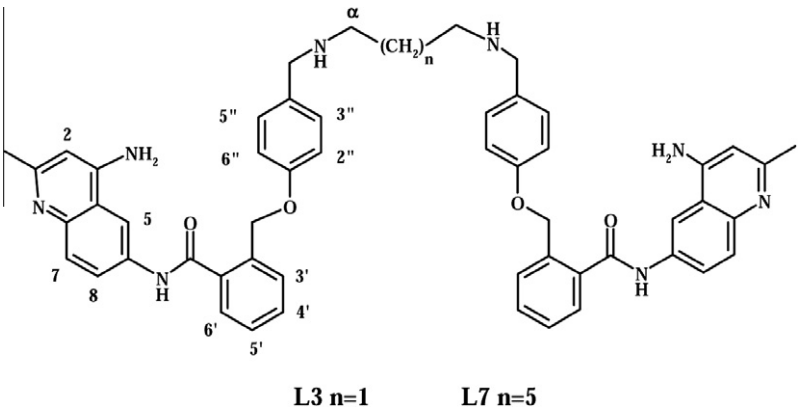

Fig. 1. Chemical structure of the bivalent NOP receptor ligands.

controller and *z* gradient coils for 32 scans at 308 K, water was suppressed by presaturation. 2D NOESY experiments were collected at 1 K × 256 data points, for mixing time varying from 50 to 300 ms, 48 scans were collected for each mixing time, water was suppressed by presaturation, spectra were processed by sine bell function and zero filled to 512 in the t1 dimension.

Cross peaks were classified as strong, medium, weak and very weak using the orto phenolic H2″H6″–H3″H5″ NOE as a reference for a strong NOE corresponding to fixed proton distance of 2.44 Å.

2.4.2. NMR experiments in the presence of liposomes

An appropriate volume of the ligand dissolved in DMSO-d_6 was added to a suspension of liposomes in 10 mM deuterated phosphate buffer to reach a final concentration of 0.5 mM ligand in 10:90 DMSO-d_6/phosphate buffer. The ligand was maintained in interaction with the liposomes one night at 308 K before acquisition. 1D ^{1}H NMR spectra were acquired on a broad band Bruker Avance 700 MHz equipped with temperature controller and *z* gradient coils for 32 scans at 308 K, water was suppressed by presaturation.

2D NOESY experiments were collected at 1 K × 256 data points, for mixing time varying from 30 to 600 ms, 48 scans were collected for each mixing time, water was suppressed by presaturation, spectra were processed by sine bell function and zero filled to 512 in the t1 dimension.

Cross peaks were classified as strong, medium, weak and very weak using the orto phenolic H2″H6″–H3″H5″ NOE as a reference for a strong NOE corresponding to fixed proton distance of 2.44 Å.

2.5. Interatomic distance calculation

The inter proton distance r_{ij} was calculated from the initial NOE build-up rate I_{ij} according to the equation $r_{ij} = r_{\text{ruler}}\ (I_{\text{ruler}}/I_{ij})^{1/6}$. A distance of 2.45 Å corresponding to the ortho proton in the benzylic ring was assumed as a ruler [9].

The initial NOE build up (I_{ij}) was derived from the curve interpolating the ratios between the NOE cross peak volumes corresponding to H_i H_j and the volume of the diagonal peak of H_i at zero mixing time [8].

2.6. Molecular modelling

Molecular modelling simulation was performed on the basis of the Chem X package employing MME minimization of energy [18]. The torsion angles of the energy minimization model were determined from the lowest energy structure.

3. Results and discussion

3.1. Preliminary solubility experiments and NMR reference experiments

Both ligands displayed poor solubility in water consequently they were dissolved in a dimethylsulfoxide/phosphate buffer mixture (DMSO/PBS). We minimized the risk of micelle or liposome dissolution by using 10% amount of the organic solvent in PBS. In the presence of micelles or liposomes this solvent mixture dissolved both ligands in 0.5 mM concentration which was the minimal concentration to achieve satisfactory signal to noise ratio in 2D NMR experiments. Dissolution of same amount of free ligands for the reference solutions required at minimum 50% of DMSO as no concentration above 0.075 mM could be obtained in 10% DMSO/PBS. Since differences in solvent composition and solute concentration are awaited to influence spectral outcomes we performed investigational 1D ^{1}H NMR spectra of ligand samples at 0.075, 0.1, 0.3 and 0.5 mM concentrations in a 10–50% range of DMSO-d_6/phosphate buffer solvent. All NMR spectra resulted perfectly superimposable evidencing neither solvent effect nor variations

Table 1
Chemical shifts assignation of L3 and L7 in the reference system 1:1% DMSO-d_6/deuterated acqueous phosphate buffer 10 mM at pH 7.2. TSP 0.5 mM was used as reference. Assignation was based on signal multiplicity and coupling constants in the 1D spectra and on 2D COSY, NOESY and TOCSY experiments. NMR assignations of the ligands in the presence of DPC were reported only for protons which displayed substantially different chemical shift in respect to the reference. NMR assignations of the ligands in the liposome environment displayed the same trend as the reference and were not reported.

Protons	NMR spectral data in the reference system	
	L3	L7
	Chemical shift, multiplicity, integral, coupling constant, diagnostic 2D cross peaks	
H5	8.13, s, 2H, $J_{5,7}$ = 1.8 Hz	8.13, s, 2H, $J_{5,7}$ = 1.9 Hz
H7	7.73, dd, 2H, $J_{7,5}$ = 1.8 Hz, $J_{7,8}$ = 9.1 Hz	7.74, dd, 2H, $J_{7,5}$ = 1.9 Hz, $J_{7,8}$ = 9.1 Hz
H8	7.69, d, 2H, $J_{8,7}$ = 9.1 Hz	7.70, d, 2H, $J_{8,7}$ = 9.1 Hz
H6′	7.65, d, 2H, $J_{6',5'}$ = 7.1 Hz	7.66, d, 2H, $J_{6',5'}$ = 6.4 Hz
H3′, H4′,H5′	7.59–7.53, m, 6H, NOE cross peak between H3′ and OCH_2	7.62–7.53, m, 6H, NOE cross peak between H3′ and OCH_2
H3″,H5″	7.01, d, 4H, COSY cross peak with H2″,H6″	7.18, d, 4H, COSY cross peak with H2″,H6″
H2″,H6″	6.87, d, 4H, COSY cross peak with H2″,H6″	6.92, d, 4H, COSY cross peak with H3″,H5
H3	6.56, s, 2H, NOE cross peak with 2-CH_3	6.56 , s, 2H, NOE cross peak with 2-CH_3
OCH_2	5.27, s, 4H, NOE cross peak with H2″,H6″,H3′	5.28, s, 4H, NOE cross peak with H2″,H6″, H3′
Benzyl-$NHCH_2$	3.58, s, 4H, NOE cross peak with H3″,H5″p0-	3.62, s, 4H, NOE cross peak with H3″,H5″
Chain NH–CH_2–CH_2	2.49, t, 4H, TOCSY and NOE cross peak with $NHCH_2$–CH_2	2.39, m, 4H, COSY and NOE cross peak with $NHCH_2$–CH_2
2-CH_3	2.44, s, 6H, NOE cross peak with H3	2.44, s, 6H, NOE cross peak with H3
Chain $NHCH_2$–CH_2	1.63–1.55, m, 2H, COSY and NOE cross peak with NH–CH_2–CH_2	1.38–1.31, m, 4H, COSY and NOE cross peak with NH–CH_2–CH_2 and $NHCH_2$–CH_2–$(CH_2)_2$
Chain $NHCH_2$–CH_2–$(CH_2)_2$–	–	m, 6H, 1.47–1.06 COSY and NOE cross peak with NH–CH_2–CH_2
	NMR spectral data in DPC solution	
	L3	L7
H5	8.21, d, 2H, $J_{5,7}$ = 1.8 Hz, TOCSY cross peak with H7	8.33, bs, 2H, TOCSY cross peak with H7
H8	8.11, bs, 2H, TOCSY cross peak with H7	8.19, d, 2H, TOCSY cross peak with H7
H6′	7.86, d, 2H, $J_{6',5'}$ = 6.2 Hz	7.90, bs, 2H
H7	7.74, d, 2H, $J_{8,7}$ = 9.2 Hz, TOCSY cross peak with H5 and H8	7.82, d, 2H, $J_{8,7}$ = 9.8 Hz, TOCSY cross peak with H5 and H8
H3′	7.59, d, 2H, $J_{3',4'}$ = 6.6 Hz NOE cross peak between H3′ and OCH_2	7.65 bs, 2H NOE cross peak between H3′ and OCH_2
H4′H5′	748–7.44, m, 4H,	7.58–7.51 m, 4H

in the supramolecular organization or self-aggregation phenomena of L3 and L7 in the different experimental conditions. These results confirmed that spectra of ligands 0.5 mM in 50% DMSO-d_6/phosphate buffer were suitable references and that any variations depended on the presence of the membrane models.

Ligand proton resonances were unambiguously assigned by 2D COSY, TOCSY and NOESY experiments (Table 1).

In 2D NOESY reference spectra, only predictable cross peaks attributable to neighbouring protons were evidenced. All cross peaks were of the same sign of the diagonal (Fig. 2); maximum NOE was observed for mixing times longer than 500 ms and no NOE effect could be detected for mixing times shorter than 200 ms with the exception of the ortho phenolic system. At comparable operating conditions, null point for the proton NOE is expected for molecules weighting 1300 Da [19]. Accordingly NMR data evidenced that both ligands tumbled in solution surrounded by a shell of solvent and/or water molecules and that they were in the slow tumbling regime.

In conclusion NMR experiments of both ligands in DMSO/phosphate buffer system portrayed highly solvated molecules with conformational flexibility probably tumbling in a preferential stretched conformation.

3.2. Experiments with micelles

1D ^{1}H NMR spectra were acquired and superimposed to a reference spectrum of each ligand.

In these series of experiments L3 and L7 displayed similar behaviour. The chemical shifts of both ligands appeared influenced by the change of environment and tended to move downfield in the presence of DPC. Mostly affected protons were quinoline H5 (about 80 Hz shift for L3, L7) and H8 (266 Hz shift for L3 and 174 Hz shift for L7) and toluic H6′ (about 100 Hz shift for L3). The phenolic protons were more shifted in L3 respectively showing 57 and 80 Hz shift for H2″,6″ and H3″,5″ while the same protons were shifted about 40–55 Hz in L7.

The O-benzylic methylene and H-3 experienced 57–59 Hz deshielding. Only the toluic protons H5′ and H4′ showed a shift upfield of about 40 Hz in L3 spectrum while for L7 their chemical shift remained substantially unchanged. (Figs. 3a and b and 4a and b). On the whole the ligands appeared to experiment the deshielding effect due to a polar medium more than the inner lipophilic micellar environment which is reported to induce a shielding effect [20,21]. These chemical shift variations suggested the insertion, with different depth for each ligand, of the toluic

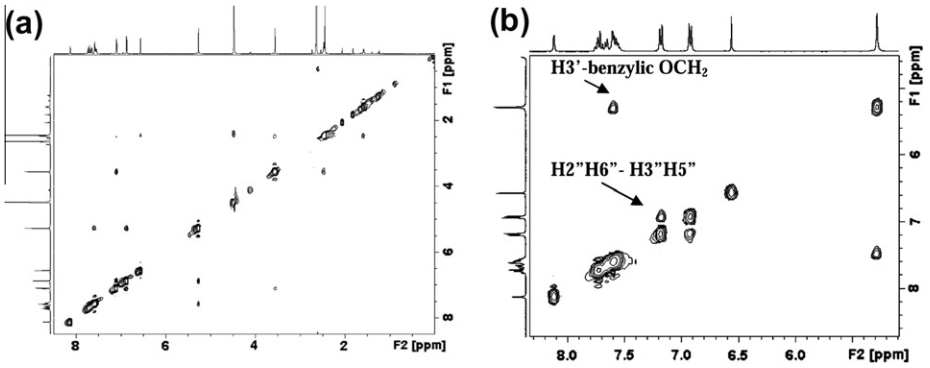

Fig. 2. (a) Total ^{1}H–^{1}H NOESY reference spectrum of L3 as an example. Expected cross peaks from neighbouring protons in the chemical structure are detectable. (b) Expansion of the aromatic region of the ^{1}H–^{1}H NOESY reference spectrum of L7 highlighting structural cross peaks between the orto H2″H6″–H3″H5″ phenol protons and between the toluic H3′ proton and the benzylic OCH_2. Spectra were collected at 600 ms mixing time.

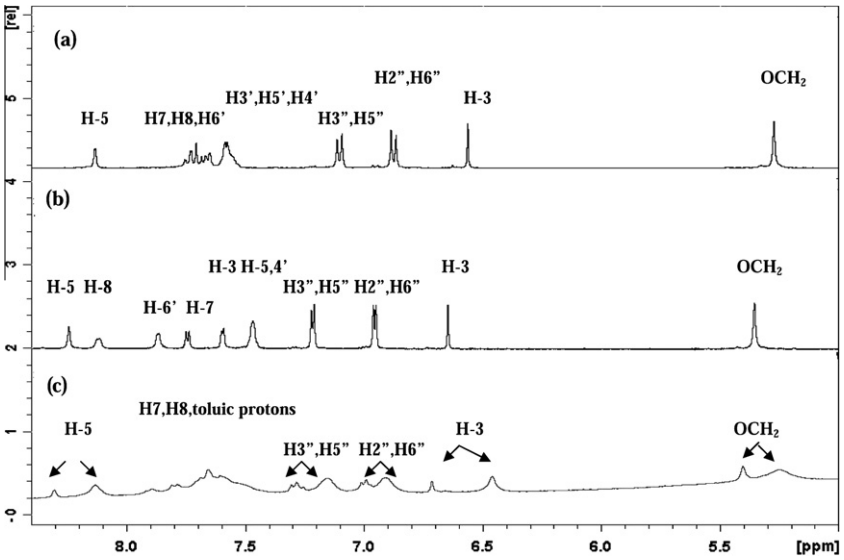

Fig. 3. Expansion of 1D ^{1}H NMR spectrum of L3. (a) Reference spectrum of L3. (b) L3 in 75 mM DPC micelles; protons are shifted downfield with the exception of the toluic group. (c) L3 in liposome environment; protons show multiple signals corresponding to different motional statuses of the ligand.

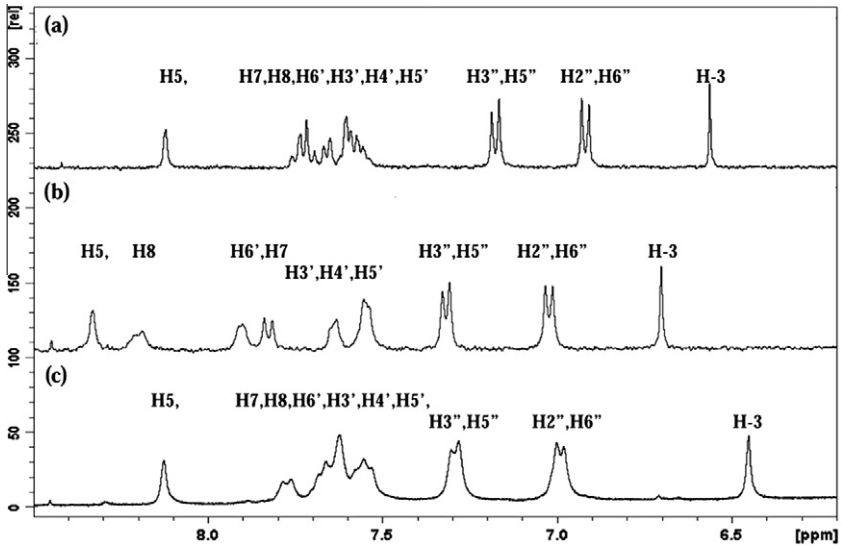

Fig. 4. Expansion of 1D ^{1}H NMR spectrum of L7. (a) Reference spectrum of L7. (b) L7 in 75 mM DPC micelles: protons tended to be shifted downfield with the exception of the toluic H3′, H5′ and H6′ (c) L7 in liposome environment: no definite trend in chemical shift variation was observed. In the presence of the cellular membrane models the protons signals were broadened as a consequence of the interaction with the macromolecules.

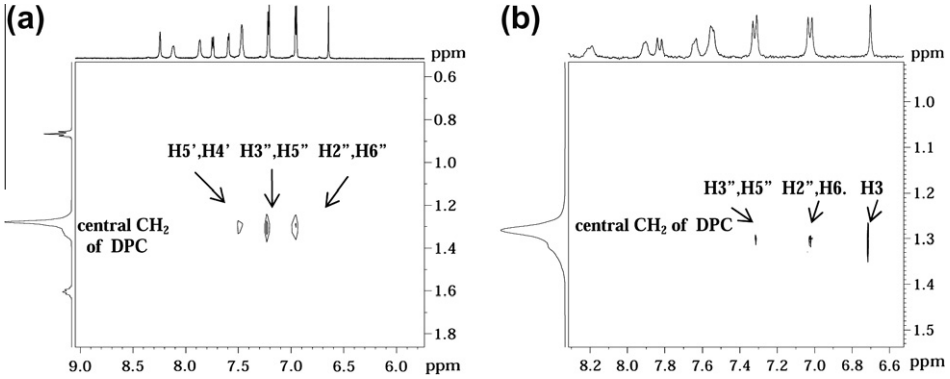

Fig. 5. Expansions of the 2D NOESY of the ligands in 75 mM DPC micelles environment. (a) Weak cross peaks are detectable between the toluic H5′,H6′, phenolic protons of L3 and the central CH_2 of the dodecyl DPC chain. (b) Very weak cross peaks are detectable between the phenolic protons and H5 of L7 and the central CH_2 of the dodecyl DPC chain.

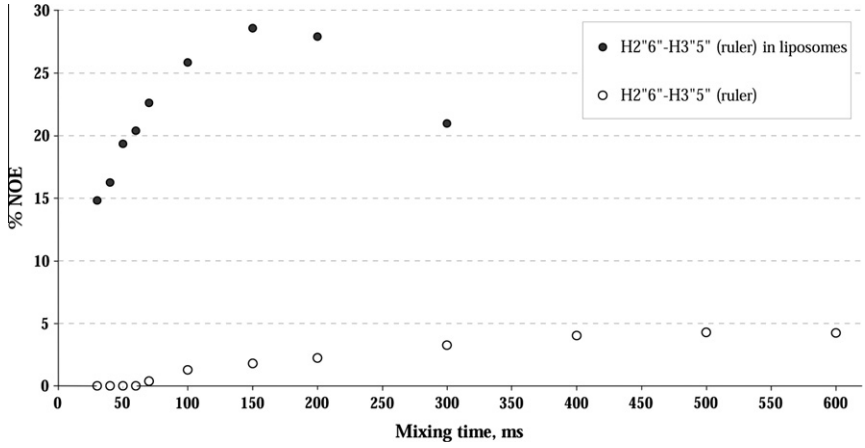

Fig. 6. Percentage of growth of ^{1}H NOE for phenol H2″6″–H3″5″ protons vs. NOESY mixing time. NOE of H2″6″–H3″5″ protons in the reference spectrum showed a lower NOE effect which reached its maximum at a mixing time of 500 ms.

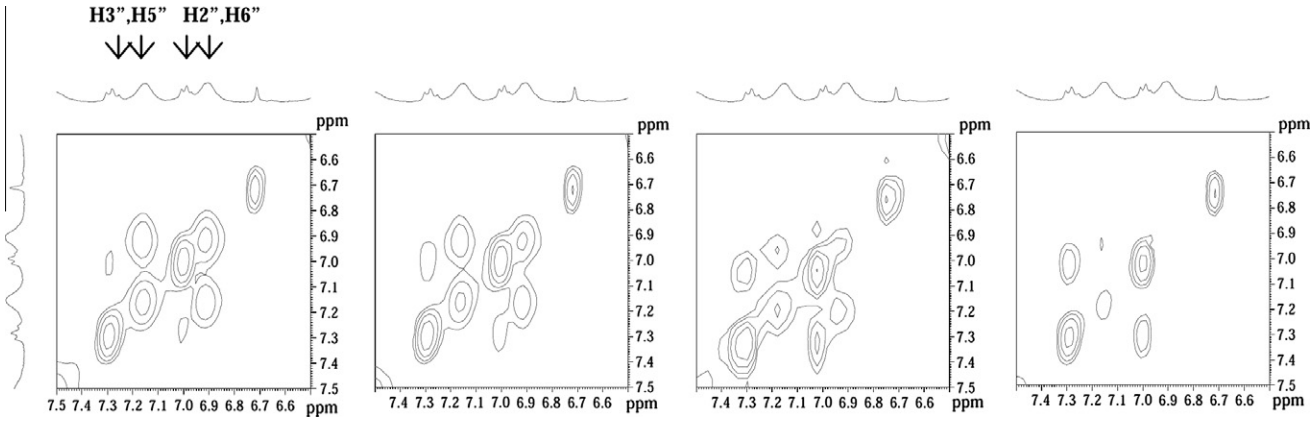

Fig. 7. 2D NOESY in liposomes environment. Selected expanded regions of the phenolic portion from L3 spectrum at 70, 100, 200 and 300 ms mixing times (from left to right). NOE cross peaks from broader signals appear at shorter mixing times.

moieties in the lipid layer hydrophobic core, with the ligand main body positioned on micelle surface near the phospholipid polar heads.

2D NOESY experiments were run at 70 ms mixing time to avoid unwanted cross peaks from magnetization transfer due to spin diffusion [22]. Micelles and ligands cross peaks were detected between the central CH_2 of the dodecyl chain and the toluic and phenolic portion of L3 and between the phenolic ring and the quinoline H3 of L7. On a qualitative interpretation cross peaks resulted weak or very weak matching an interproton distance of about 5–6 Å [23] (Fig. 5a and b).

The presence of NOESY cross peaks between the micelle hydrophobic core protons and the toluic and phenolic ones is in good accord with the hypothesis formulated on the basis of chemical shift variations that pictured the ligands approaching the inner lipophilic layer by the aromatic rings though remaining in the external environment. No novel structural NOE cross peaks were detectable and moderate broadening of the ligands resonances in the presence of micelles was observed. Overall data supported the hypothesis that the association with the micelles is not distorting the conformation of the ligands, that maintained flexibility or a preferential stretched conformation.

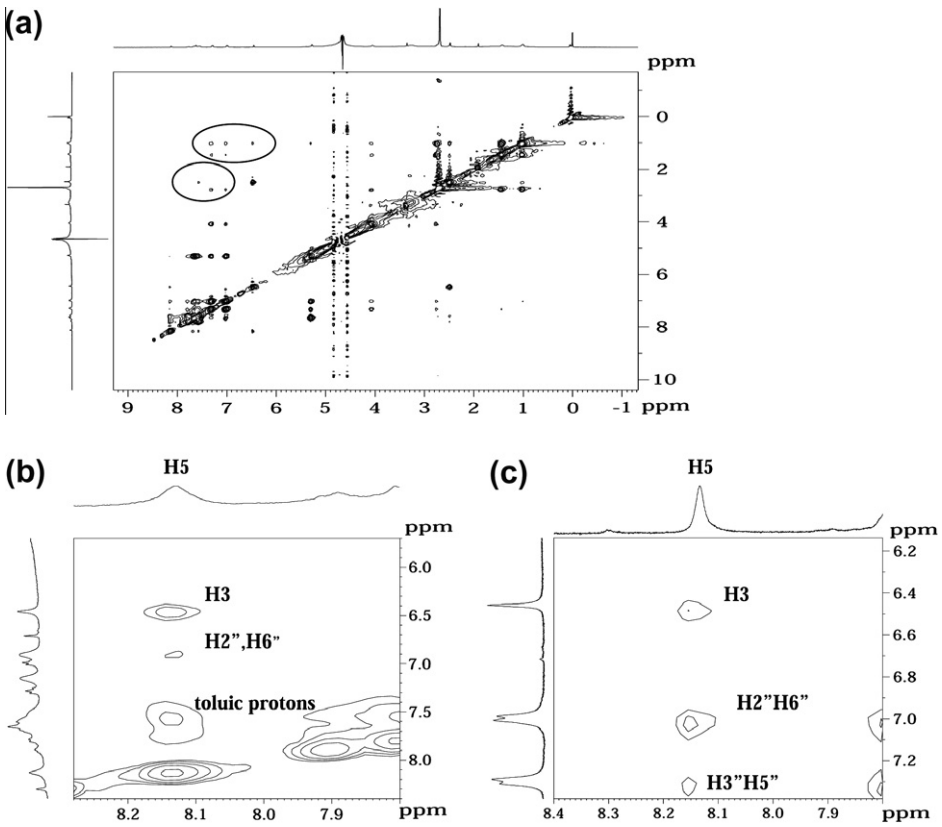

Fig. 8. 2D NOESY of the ligands in liposomes environment. (a) Total view of the spectrum of L7 reported as an example. Circled cross peaks evidenced neighborhood of L7 quinolinic and phenolic portions to liposome methylenes and trimethylammonium heads. (b) Expansion of the H5 zone highlighting L3 inner cross peaks between H5 and H3 and between H5 and the toluic portion. (c) Expansion of the H5 zone highlighting L7 inner cross peaks between H5 and H3 and between H5 and the phenolic portion.

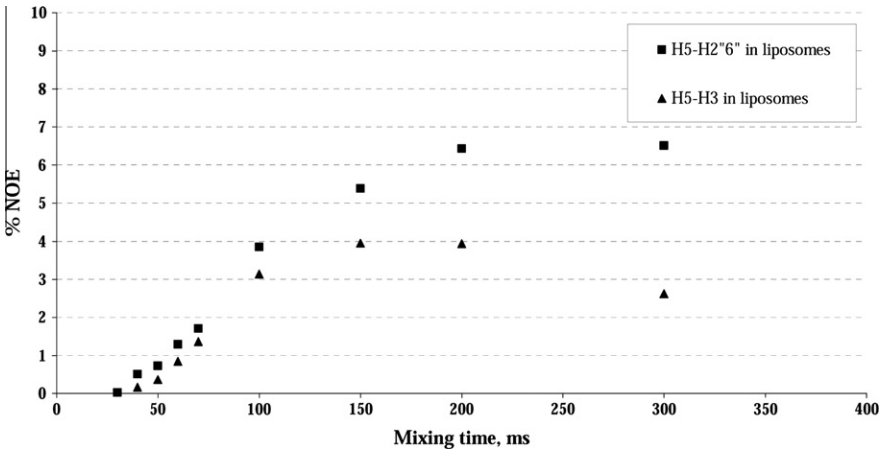

Fig. 9. NOE build up curves. Percentage of growth of NOE for L7 protons in the presence of liposomes showed maximum value at mixing time of 150 or 200 ms.

3.3. Experiments with liposomes

Experiments with liposomes led to the most remarkable results. Data from 1D NMR and 2D NOESY suggested strong interaction with the liposomes.

In 1D NMR spectra proton signals showed no definite trend in chemical shift variations and were strongly broadened in respect to the reference spectra (Figs. 3a and c and 4a and c). Band broadening is correlated to the shortening of transverse relaxation time (T_2) of ligands according to the relation $\Delta v = k/\pi T_2$ [24]. This was indicative of rigidness of the structure and was attributable to the interactions with the liposomes.

Moreover L3 spectrum showed multiple signals of very different width in correspondence of the same proton. This indicated that L3 molecules coexisted in at least two motional statuses in the liposome environment. The more shielded group of signals displayed about 40 Hz width and could be assigned to the molecules that were deeply trapped within the lipophilic medium. This highly interacting form of L3 showed from seven to ninefolds enlargement of the O-benzylic and *N*-benzylic methylenes and 2-CH_3, about six times enlargement of H-3 while signals of the other aromatic protons tended to broaden two or threefold.

L7 protons signals mainly doubled their width in the liposome environment. This effect was more pronounced for the quinoline H3 and 2-CH_3, whose signals enlarged threefold. 2D NOESY spectra with mixing times of 30, 40, 50, 60, 70, 100, 150, 200 and 300 ms were collected in order to observe the evolution of cross peaks intensity and detect the maximum dipolar correlation for all molecular moieties of both ligands. In conformity with the information from 1D NMR data, internal structural NOE of H2″6″–H3″5″ protons were detectable at shorter mixing times than in NOESY reference experiments (Fig. 6). This suggested a slower reorientation dynamic of the ligands which appeared to assume the motion of the liposomes. The motional status of the two forms of L3 molecules could be evidenced by the 2D NOESY pattern at different mixing times. The more enlarged rigid molecules showed strong NOE effect at short mixing times (below 70 ms) and gradually lost it when the NOE cross peaks of the more flexible molecules appeared (100 ms) (Fig. 7). Interaction between L3 and L7 and the liposomes was confirmed by weak cross peaks between the quinoline and phenolic portion of the ligands and the protons of the phospholipidic chain at 1.0 and 1.5 ppm and of the trimethylammonium head at 3.2 ppm (Fig. 8a). Most interestingly previously unseen cross peaks of the ligands protons were identified between the quinoline H3 and H5 and between the quinoline H5 and the phenolic protons (Fig. 8b and c). These signals supported the hypothesis of a conformational change of the ligands in presence of liposomes. Only a qualitative analysis of the 2D NOESY spectra of L3 was possible as the multiple forms of the ligands made cross peaks quantification unreliable. On the basis of NOESY data quinoline H3 and H5 approached about 3 Å to each other and the quinoline H5 neighboured the phenol ring at a 5 Å distance. NOEs are indicative of a prevalent folded conformation displacing the quinoline arms over each other.

Since L7 spectra did not show the multiple forms observed in L3 experiments, quantitative NOE build up calculations could be carried out with good reliability [25]. Within the range of observed mixing times (30, 40, 50, 60, 70, 100, 150, 200 and 300 ms) NOE increase is linear with time and proportional to the sixth power of the inter-protonic distance (r_{ij}^6) [8]. For mixing times longer than 100 ms NOE build up curves deviated from linearity because of diffusion phenomena as awaited in liposome systems (Fig. 9). NOE data of H5, H3 and the phenolic protons indicated that the quinoline and the phenol of the same pharmacophoric unit approached within a distance of 4 Å and that the two quinoline rings approached at about 3 Å. Therefore also in the case of L7 the conformational properties of the ligand are greatly influenced by the liposomes. As it was seen for L3, the ligand seemed to be preferentially curled in the presence of liposomes.

3.4. Molecular modelling calculations

Restrains from NOESY were applied to molecular modelling calculation and minimization of conformational families was performed to find out the preferential conformations. In liposomes the ligands appeared to assume a prevalent bent conformation (Fig. 10).

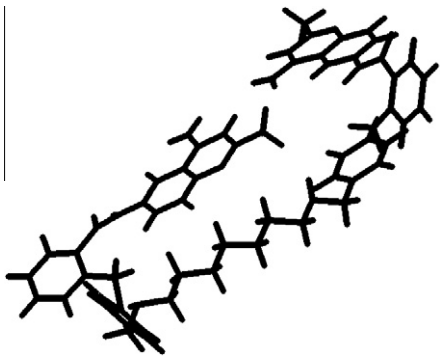

Fig. 10. Energy-minimized conformation of L7 in the liposomes system.

4. Conclusion

The preferential conformations of the bivalent NOPr ligands L3 and L7 were determined as free, in DPC micelles solution and in a DMPC/cholesterol liposomes system. Results indicated significant interaction of both ligands with the membrane models and suggested a preferential folded conformation of the ligands that is accountable to their interaction with the liposomes. Structural differences in the linker chain lengths affected the degree of interaction of the ligands with the liposomes. Studies on L7 indicated one highly favourite interacting conformational population, whereas investigations on L3 showed more than two interacting conformational populations displaying different degrees of mobility. Such differences could be ascribed to the dissimilar lipophilicity of the ligands. It is worth noting that the ligands assumed a rounded shape in interaction independently from the length of their linking chain.

The usefulness of this study relies on the information retrieved on the structural modifications relevant to future syntheses of analogous compounds. The structure here investigated could be further developed to achieve selectivity between central and peripheral NOPr activations in respect to the monomer. Results indicated potential BBB good permeation of the dimer ligands. Moreover, this study suggested that hardening of the linker by insertion of amidic group could be a valid option for the possible interaction with dimer receptors. In fact L3 and L7 folded conformation could prevent extension of the ligands between different subreceptorial units. To gain further information on the interactions between these ligands or analogous molecules and the opioid receptors work is in program to upgrade the NMR study to cellular membranes.

Acknowledgment

We are grateful to Mr. Tonino Puccio for technical assistance.

References

[1] C. Mollereau, M. Parmentier, P. Mailleux, J.L. Butour, C. Moisand, P. Chalon, D. Caput, G. Vassart, J.C. Meunier, FEBS Lett. 341 (1994) 33–38.
[2] D.G. Lambert, Nat. Rev. Drug Discov. 7 (2008) 694–710.
[3] P.S. Portoghese, J. Med. Chem. 44 (2001) 2259–2269.
[4] I. Berque-Bestel, F. Lezoualch, R. Jockers, Curr. Drug Discov. Technol. 5 (2008) 312–318.
[5] J.M. Contreras, J.J. Bourguignon, in: C.G. Wermuth (Ed.), The Practice of Medicinal Chemistry, Academic Press, London, 2003, pp. 251–273.
[6] J. Guo, S. Pavlopoulos, X. Tian, D. Lu, S.P. Nikas, D.P. Yang, A. Makriyannis, J. Med. Chem. 46 (2003) 4838–4846.
[7] Y. Xu, V.E. Yushmanov, P. Tang, Biosci. Rep. 22 (2002) 175–196.
[8] B. Xiang, G.D. Markham, J. Biol. Chem. 271 (1996) 27531–27535.
[9] D. Neuhaus, M.P. Williamson, The Nuclear Overhauser Effect in Structural and Conformational Analysis, Wiley-VCH, New York, 2000.
[10] H. Shinkai, T. Ito, T. Iida, Y. Kitao, H. Yamada, I. Uchida, J. Med. Chem. 43 (2000) 4667–4677.
[11] H. Yamada, H. Nakamoto, Y. Suzuki, T. Ito, K. Aisaka, Br. J. Pharmacol. 135 (2002) 323–332.
[12] I. Sestili, A. Borioni, C. Mustazza, A. Rodomonte, L. Turchetto, M. Sbraccia, D. Riitano, M.R. Del Giudice, Eur. J. Med. Chem. 39 (2004) 1047–1057.
[13] L.B.L. Hansen, B.D. Larsen, C. Thorkildsen, C.B. Knudsen (Clark & Elbing LLP), USP 0287478 A1, 2008.
[14] D.D. Lasic, Bull. Magn. Reson. 13 (1991) 3–13.
[15] M.R. Del Giudice, A. Borioni, G. Bastanzio, C. Mustazza, I. Sestili, Eur. J. Med. Chem., submitted for publication.
[16] S.J. Marrink, D.P. Tieleman, A.E. Mark, J. Phys. Chem. B 104 (2000) 12165–12173.
[17] R.E. Stafford, T. Fanni, E.A. Dennis, Biochemistry 28 (1989) 5113–5120.
[18] M.C. Nicklaus, G.W. Milne, D. Zaharevitz, J. Chem. Inf. Comput. Sci. 33 (1993) 639–646.
[19] W.E. Hull, in: W.R. Croasmun, R.M.K. Carlson (Eds.), Two Dimensional NMR Spectroscopy: Application for Chemists and Biochemists, Wiley-VCH, New York, 1994, pp. 67–456.
[20] E.Y. Chekmenev, S.K. Chow, D. Tofan, D.P. Weitekamp, B.D. Ross, P. Bhattacharya, J. Phys. Chem. B 112 (2008) 6285–6287.
[21] L. Fernandes Fraceto, A. Spisni, S. Schreier, E. De Paula, Biophys. Chem. 115 (2005) 11–18.
[22] D. Huster, K. Gawrisch, J. Am. Chem. Soc. 121 (1999) 1992–1993.
[23] N.E. Jacobsen, NMR Spectroscopy Explained: Simplified Theory, Applications and Examples for Organic Chemistry and structural Biology, Wiley, Hoboken New Jersey, 2007. pp. 250–252.
[24] T.H. Schmitt, Z. Zheng, O. Jardetzky, Biochemistry 34 (1995) 13183–13189.
[25] R.P. Meadows, K. Kaluarachchi, C.B. Post, D.G. Gorenstein, Bull. Magn. Reson. 13 (1991) 22–48.